



Synthesis, vibrational spectral and nonlinear optical studies of N-(4-hydroxy-phenyl)-2-hydroxybenzaldehyde-imine: A combined experimental and theoretical investigation

Yufeng Wang^a, Zongxue Yu^{a,c}, Yuxi Sun^{a,b,*}, Yishi Wang^a, Lude Lu^a

^a Key Laboratory for Soft Chemistry and Functional Materials of Education Ministry, Nanjing University of Science & Technology, Nanjing 210094, PR China

^b Key Laboratory of Life-Organic Analysis, School of Chemistry & Chemical Engineering, Qufu Normal University, Qufu, 273165, PR China

^c School of Chemistry & Chemical Engineering, Southwest Petroleum University, Chengdu, 610500, PR China

ARTICLE INFO

Article history:

Received 11 February 2011

Received in revised form 11 April 2011

Accepted 1 May 2011

Keywords:

Imine compound

Synthesis

Vibrational spectra

DFT

NLO

ABSTRACT

The study of imine-bridged organics has been the one hot spot of photo-responsive material sciences in recent years. Herein we make a study of the synthesis, characteristics and potential application of N-(4-hydroxy-phenyl)-2-hydroxy-benzaldehyde-imine (HPHBI), C₁₃H₁₁NO₂. The studied compound was synthesized in one step by the condensation reaction of salicylaldehyde and 4-aminophenol in methanol solution, and characterized by single crystal X-ray diffraction, FT-IR and FT-Raman techniques with theoretical calculations at B3LYP/6-31G(d) level. The molecule adopts *trans* configuration about central C=N bond with intramolecular hydrogen bonding, and the adjacent molecules form wave-shaped structure linked by strong intermolecular hydrogen bonding mechanism along *b* axis. The vibrational spectra have been precisely assigned with the aid of theoretical frequencies. Furthermore, the thermodynamic properties have been obtained by the theoretical vibrational analysis for HPHBI. The total linear polarizability and first-order hyperpolarizabilities calculated on the studied compound respectively present 25.378 Å³ and 1.655 × 10⁻²⁹ cm⁵/esu, which indicates the compound has relatively good nonlinear optical property.

© 2011 Elsevier B.V. All rights reserved.

1. Introduction

Recently, the heterojunction organics have attracted increasing attention due to their potential applications in optical communications, optoelectronic materials, biofunctional compounds, especially, excellent nonlinear optical (NLO) responses [1–7]. As we know that the heterojunction units are the core structures of a number of natural products as amine acids, DNA, bioelectric or photovoltaic materials. Schiff bases have been proved to be a class of functionally active compounds. For example, Hadjoudis et al. have found that some Schiff base compounds exhibit thermochromism or photochromism properties [8]. Ünver et al. have reported the structural and NLO properties for some imine-bridged aromatic compounds [1,7,9]. Our group has been engaged in the study of the synthesis and NLO properties of a series of imine-bridged antipyrine derivatives for several years [3–6,10–13].

Generally, organic compounds with aromatic moieties can easily transport electrons or charges via/among their conjugated segments to perform photoelectric or NLO effects. Currently, the

organics with electron-donating and electron-withdrawing groups have been regarded as an interesting kind of NLO compounds better than inorganic materials [1,14], wherein, the imine-bridged benzene derivatives have shown high optical nonlinearities. As a result, these compounds are of considerable current research interest in the photo-responsive materials in recent years.

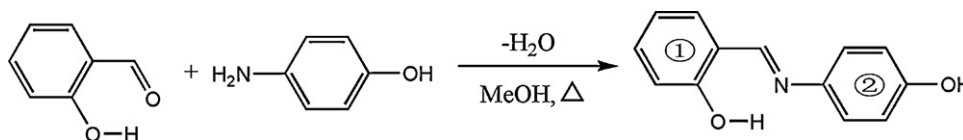
As a heterojunction model compound, N-(4-hydroxy-phenyl)-2-hydroxy-benzaldehyde-imine (HPHBI) (Scheme 1) was synthesized and characterized by X-ray crystal diffraction, FT-IR, FT-Raman techniques, furthermore, the thermodynamic and NLO properties of the studied compound were obtained by theoretical calculations at B3LYP/6-31G(d) level in this work.

2. Experimental

2.1. Synthesis of the title compound

Most of the chemicals (reagent grade) in this work were purchased from Alfa or Ronghua chemical Corp. and used without further purification. The title compound was synthesized in one step according to the classical condensation of aldehyde and ammonia, and the reaction path is shown in Scheme 1. Salicylaldehyde and 4-aminophenol with an equal mole ratio were dissolved in

* Corresponding author. Tel.: +86 25 84303229; fax: +86 25 84315054.
E-mail address: yuxisun@163.com (Y. Sun).



Scheme 1. Synthetic route for HPHBI.

methanol solution. The reaction mixture was stirred for about an hour under reflux to give an orange clear solution. After allowing the solution to stand in air for 11 d, orange block-shaped crystals had formed at the bottom of the vessel on slow evaporation of the solvent (yield 84.7%).

2.2. FI-IR and FT-Raman measurements

The FT-IR spectra of solid compound was recorded in the range of 4000–400 cm^{-1} in evacuation mode with a scanning speed of 30 $\text{cm}^{-1} \text{min}^{-1}$ and a spectral width of 2.0 cm^{-1} on a Bruker IFS 66V FI-IR spectrometer using KBr pellet technique.

The FT-Raman spectrum of HPHBI was measured on RENISHAM inVia Raman microscope equipped with a counter current detector and a diode laser (785 nm line of Nd-YAG laser as excitation wavelength) in the region 4000–100 cm^{-1} with a spectral resolution of 1.0 cm^{-1} in the backscattering configuration.

2.3. X-ray determination

A suitable single crystal was attached to a glass fiber. Data were collected at 295(2) K on a Bruker AXS SMART APEX area-detector diffractometer (Mo $K\alpha$ radiation, $\lambda = 0.71073 \text{ \AA}$) with SMART [15] as a driving software; data integration was performed by SAINT-Plus software [16] with multiscan absorption correction applied using SADABS [17]. The crystal structure was solved by a direct method based on difference Fourier and refined by least squares on F^2 with anisotropic displacement parameters for non-H atoms. All of H atoms attached to C/O were placed in calculated positions. All the calculations to solve the structure, to refine the proposed model, and to obtain the derived results were carried out with the computer programs of SHELXS-97 [18], SHELX-L97 [18] and SHELXTL [19]. Full use of CCDC package was also made for searching in the CSD database.

3. Theoretical

In this work, the quantum chemical study was used to make definite assignments for the fundamental normal modes, and to clarify the experimental FT-IR and FT-Raman spectral bands, and to give additional thermodynamic functions and nonlinear optical properties for the title compound.

For meeting the requirements of accuracy and economy, the theoretical method and basis set should be considered firstly. The density functional theory (DFT) has been proved to be extremely useful in treating electron relativities, and the basis set of 6-31G(d) has been used as a very effective and economical level for many organic molecules [20]. Based on the points, the density functional Becke3–Lee–Yang–Parr (DFT/B3LYP) with standard 6-31G(d) basis set was adopted to compute the properties of the studied compound in this work. All the calculations were performed using Gaussian 03W program package [21] with the default convergence criteria.

For the investigated molecule, the initial geometrical configuration was generated from its X-ray diffraction (XRD) crystallographic data, and the optimized geometry corresponding to the minimum on the potential energy surface was obtained by solving self-consistent field equation iteratively without any constraints. The

harmonic vibrational frequencies were analytically calculated by taking the second order derivative of energy using the same level of theory. Normal coordinate analysis was performed to obtain full description of the molecular motion pertaining to the normal modes using the GaussView program [22]. Simultaneously, the statistical thermodynamic functions were theoretically predicted by the harmonic frequencies of the optimized structures for the title compound.

The Raman scattering activities (S_i) calculated by Gaussian 03W program were suitably converted to relative Raman intensities (I_i) using the following relationship derived from the basic theory of Raman scattering stated in previous Refs. [23,24]:

$$I_i = \frac{f(\nu_0 - \nu_i)^4 S_i}{\nu_i [1 - \exp(-hc\nu_i/kT)]} \quad (1)$$

where ν_0 is the exciting frequency (in cm^{-1} units), ν_i is the vibrational wavenumber of the i th normal mode, h , c and k are universal constants, and f is the suitably chosen common scaling factor for all the peak intensities.

The nonlinear optical (NLO) properties can be obtained by the previously stated methods [13,25–35]. In this work, using the x , y , z components, the total static dipole moment (μ_0), linear polarizability (α_0) and first-order hyperpolarizability (β_0) are calculated by the following equations defined in previous Refs. [13,31–34]:

$$\mu_0 = \sqrt{\mu_x^2 + \mu_y^2 + \mu_z^2} \quad (2)$$

$$\alpha_0 = \frac{\alpha_{xx} + \alpha_{yy} + \alpha_{zz}}{3} \quad (3)$$

$$\beta_0 = \sqrt{(\beta_{xxx} + \beta_{xyy} + \beta_{zzz})^2 + (\beta_{yyy} + \beta_{xxy} + \beta_{yzz})^2 + (\beta_{zzz} + \beta_{xzx} + \beta_{yyz})^2} \quad (4)$$

4. Results and discussion

4.1. Geometric structure

The molecular structure of HPHBI with the atom-numbering scheme is shown in Fig. 1. X-ray single crystal structure determination indicates the cell structure of the title compound contains eight independent structural units belonging to monoclinic system with space group of $C2/c$. So, the molecule packing structure belongs to the C-face central lattice with one diadaxis along b axis and one glide reflection plane along c axis (Fig. 2(a)), which is different from the reported crystal parameters [36]. The crystallographic data and

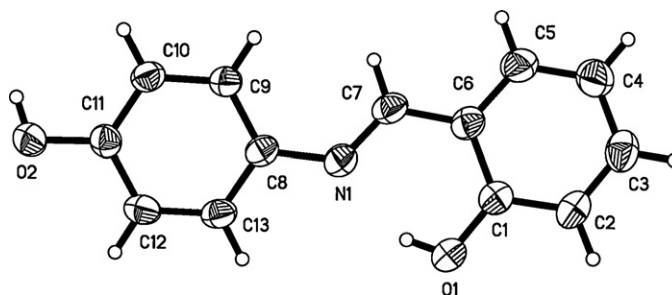


Fig. 1. The molecular structure of HPHBI. The displacement ellipsoids are plotted at the 30% probability level.

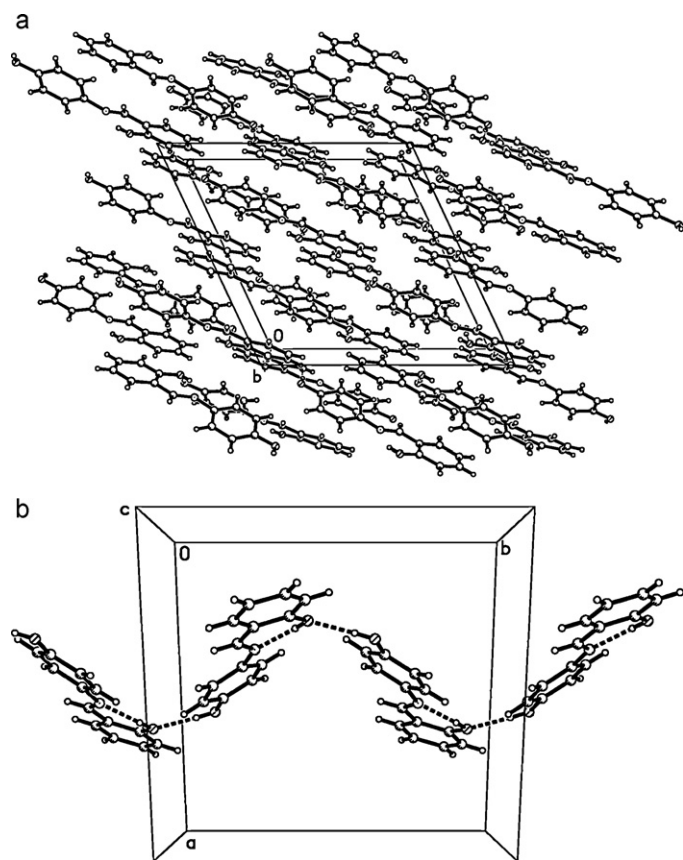


Fig. 2. Neighboring molecular diagrams of HPHBI: (a) molecular packing viewed along *b* axis, (b) hydrogen-bonding viewed along *c* axis.

experimental details for the studied compound are summarized in Table 1.

The selected bond lengths, bond angles and torsion angles are listed in Table 2. In the compound, the N1–C7 distance of 1.288 (4) Å is consistent with the corresponding values in similar Schiff's base ligands [1,4,5,13,37]. The imine-bridged benzene rings form an effective torsion angles of 14.9 (4)°, which is slightly more than the values of the imine-bridged ring torsion angles of antipyrine Schiff base compounds [4,5,13].

Table 1
Crystallographic and experimental data for HPHBI.

Compound	C ₁₃ H ₁₁ NO ₂
Formula weight	213.23
Color/shape	Orange/Block
Crystal structure	Monoclinic
Space group	C2/c
Cell parameters	
<i>a</i> (Å)	13.338 (2)
<i>b</i> (Å)	12.985 (2)
<i>c</i> (Å)	13.824 (2)
β (°)	115.105 (2)
<i>V</i> (Å ³)	2168.1 (6)
<i>Z</i>	8
Density(g/cm ³)	1.307
θ Range for data collection(°)	2.3–23.0
θ_{\max} (°)	25.5
Index ranges	$-16 \leq h \leq 16; -15 \leq k \leq 15; -16 \leq l \leq 16$
Measured reflections	7975
Independent reflections	2015
Reflections with $I > 2\sigma(I)$	1460
$\Delta\rho_{\max}, \Delta\rho_{\min}$ (e Å ⁻¹)	0.66, -0.15
(Δ/σ) _{max}	0.0001
CCDC	808948

Table 2
Selected bond lengths (Å), bond angles (°) and torsion angles (°) for HPHBI.

Compound	Experimental	Theoretical
Bond length (Å)		
O1–C1	1.316 (3)	1.342
O2–C11	1.353 (4)	1.367
N1–C8	1.416 (4)	1.407
N1–C7	1.288 (4)	1.293
C1–C6	1.422 (4)	1.424
C1–C2	1.385 (4)	1.403
C2–C3	1.359 (5)	1.389
C3–C4	1.391 (6)	1.404
C4–C5	1.366 (6)	1.386
C5–C6	1.397 (5)	1.409
C6–C7	1.422 (4)	1.450
C8–C13	1.380 (4)	1.406
C8–C9	1.393 (4)	1.404
C9–C10	1.373 (4)	1.393
C10–C11	1.387 (4)	1.399
C11–C12	1.390 (4)	1.400
C12–C13	1.372 (4)	1.388
Bond angles (°)		
C7–N1–C8	126.4 (2)	121.7
O1–C1–C6	120.5 (2)	122.1
C2–C1–C6	118.6 (2)	119.4
O1–C1–C2	120.9 (2)	118.5
C1–C2–C3	121.3 (3)	120.3
C2–C3–C4	121.0 (3)	121.0
C3–C4–C5	119.0 (4)	119.1
C4–C5–C6	121.6 (3)	121.4
C5–C6–C7	120.8 (3)	119.7
C1–C6–C7	120.7 (2)	121.5
C1–C6–C5	118.6 (3)	118.8
N1–C7–C6	122.4 (2)	122.5
C9–C8–C13	118.6 (3)	118.4
N1–C8–C9	124.0 (2)	123.9
N1–C8–C13	117.4 (2)	117.7
C8–C9–C10	120.6 (2)	120.7
C9–C10–C11	120.4 (2)	120.2
O2–C11–C12	117.8 (2)	117.5
O2–C11–C10	123.0 (2)	122.8
C10–C11–C12	119.2 (3)	119.7
C11–C12–C13	119.9 (2)	119.8
C8–C13–C12	121.3 (2)	121.2
Torsion angles (°)		
C8–N1–C7–C6	176.5(3)	177.3
C7–N1–C8–C13	169.0(3)	150.7
C5–C6–C7–N1	-178.9(3)	179.6

There are two types of strong hydrogen-bonds in the molecular packing diagram (Table 3 and Fig. 2(b)). The intramolecular hydrogen bonding of O1–H1...N1 is helpful to strengthen the stability of the molecular structure and the intermolecular hydrogen bonding of O2–H2...O1ⁱ (*i*: 1/2 – *x*, -1/2 + *y*, 1/2 – *z*) is helpful to connect the adjacent molecules to form a one-dimensional wave-structural supermolecular structure along *b* axis. Therefore, the hydrogen bonds of the compound play important roles in the molecular and crystal stabilities.

The theoretical parameters for HPHBI optimized at B3LYP/6-31G(d) level are also listed in Table 2. It is observed that the experimental and theoretical geometric parameters are not completely identical owing to the fact that the molecular geometry in the gaseous phase is different from the one in the solid phase [38]. The optimized bond lengths are mostly longer than the experimental values agreeing within 0.030 Å and the optimized bond angles

Table 3
Hydrogen-bond parameters for HPHBI.

Hydrogen bonding	<i>D</i> –H(Å)	H... <i>A</i> (Å)	<i>D</i> ... <i>A</i> (Å)	<i>D</i> –H... <i>A</i> (°)
O1–H1...N1	0.800	1.840	2.553 (3)	148.00
O2–H2...O1 ⁱ	0.810	1.850	2.660 (3)	174.00

Symmetry codes: (i) 1/2 – *x*, -1/2 + *y*, 1/2 – *z*.

are slightly different from the experimental data disagreeing within 4.7° .

Although there are some differences between experimental and theoretical values, they are generally accepted that geometric parameters depend upon the method and the basis set used in the calculations, and the optimized structure can be used as a base to calculate other properties for the compound.

4.2. Vibrational spectral analysis

The studied molecular structure belongs to C_1 point group. The molecule has 27 atoms and 75 normal modes of fundamental vibrations. All the 75 fundamental vibrations with their mode numbers are obtained by theoretical calculation. According to the motion of the individual atoms with the aid of GaussView 3.0 software [22], the detailed vibrational spectral assignments have been given in Table 4 with theoretical vibrations scaled by the factor of 0.9614 for B3LYP method [39].

The IR and Raman spectra of the title compound are shown in Figs. 3 and 4, respectively. On the whole, the infrared features are more complicated than the Raman spectra for the studied compound. A detailed spectral analysis is given below in the present work.

4.2.1. C–H vibrations

The aromatic C–H stretching vibration shows in the region $3100\text{--}3000\text{ cm}^{-1}$, which is a typical vibration region for characterization of the aromatic compounds [40,41]. In the present case, the scaled C–H stretching vibrations region at $3098\text{--}3046\text{ cm}^{-1}$ (mode nos. 74–66) by B3LYP/6-31G(d) method are in excellent agreement with the FT-IR band observed at 3047 cm^{-1} . In this region, the involvement of the substitution has not much impact on the vibration of the aromatic C–H stretching.

The aromatic C–H in-plane bending vibration occurs in the range of $1290\text{--}900\text{ cm}^{-1}$ and the out-of-plane bending vibration shows in the frequency range of $999\text{--}755\text{ cm}^{-1}$ in the substituted benzene compounds [40,41]. For the studied compound, a number of the calculated C–H in-plane bending vibrations (mode nos. 50, 47 and 44–40) lie in the range of $1282\text{--}1020\text{ cm}^{-1}$, which are closed to experimental FT-IR bands at $1244, 1161, 1026\text{ cm}^{-1}$ and FT-Raman bands at $1255, 1143, 1100, 1045\text{ cm}^{-1}$. The C–H out-of-plane bending vibrations are theoretically found at $943\text{--}738\text{ cm}^{-1}$ (mode nos. 37–33, 31–30, 27–25), which also shows good agreements with the observed values of $852, 766$ and 744 cm^{-1} in FT-IR and $770, 737\text{ cm}^{-1}$ in FT-Raman.

4.2.2. Ring vibrations

The benzene ring C=C stretching vibrations generally appear in the special region of $1650\text{--}1450\text{ cm}^{-1}$ [38]. In this work, the very strong bands observed at $1593, 1531, 1487, 1463\text{ cm}^{-1}$ in FT-IR and middle to strong bands at $1596, 1525, 1357\text{ cm}^{-1}$ in FT-Raman are assigned to the aromatic C=C stretching vibrations, which are good coherence with theoretically calculated data at $1618\text{--}1322\text{ cm}^{-1}$ (mode nos. 63–56, 53–52). Generally, these modes are accompanied with the combination of the C–H in-plane bending vibrations.

The observed bands of $667, 574, 548$ and 479 cm^{-1} in FT-IR spectrum are assigned to C–C–C deformation vibrations of the phenyl rings. And the frequencies of 582 and 476 cm^{-1} in FT-Raman spectrum belong to the same vibrations. The theoretically computed C–C–C deformation vibrations show good agreements with recorded spectral data.

The No. 1 ring breathing calculated at 625 cm^{-1} (mode no. 21) correlates excellently with the observed bands of 620 cm^{-1} in FT-IR and 630 cm^{-1} in FT-Raman. The same mode for the No. 2 ring at 843 cm^{-1} (mode no. 32) is also satisfactorily coinciding with the

frequency of 852 cm^{-1} in FT-IR and 849 cm^{-1} in FT-Raman. These results are exactly consistent with reported values [40,42].

4.2.3. C–N vibrations

In general, the ready identification of C–N vibration is a really difficult task, because the mixing of several bands is possible in these regions. However, the C–N stretching assignments are identified by the animation application of GaussView 3.0 graphical interface for Gaussian output file. In the present work, a very strong band at 1633 cm^{-1} in FT-IR spectrum (1625 cm^{-1} in FT-Raman) is assigned to C=N stretching vibration, which matches the calculated value at 1621 cm^{-1} (mode no. 64). The theoretically predicted value (mode no. 46) at 1176 cm^{-1} is attributed to C–N stretching vibration with C6–C7 stretching vibration, which also goes well with the experimental value at 1224 cm^{-1} in FT-IR and 1143 cm^{-1} in FT-Raman. All these results are nearer to the data reported by Ilic [43].

4.2.4. O–H vibrations

The reported in-plane O–H bending leads to a medium to strong band in the region of $1440\text{--}1260\text{ cm}^{-1}$ [41]. In this work, the O–H in-plane bending vibration is mixed with other vibrations such as C–H in-plane bending, C–C stretching vibration and C–N stretching vibration. The calculated frequencies at $1568, 1416,$ and 1213 cm^{-1} (mode nos. 60, 55, and 47) belong to in-plane O–H bending vibrations of No. 1 ring, and the calculated frequencies of $1328, 1162\text{ cm}^{-1}$ (mode nos. 53, 45) are ascribed to in-plane O–H bending vibrations of No. 2 ring. Because of the effects of intramolecular and intermolecular hydrogen bonds, the strong peaks observed at $1593, 1418, 1161\text{ cm}^{-1}$ in FT-IR ($1579, 1255\text{ cm}^{-1}$ in FT-Raman) spectrum and the weak band at $1307, 1118\text{ cm}^{-1}$ in FT-IR spectrum are respectively assigned to in-plane O–H bending vibrations of No. 1 and No. 2 rings, respectively. As expected, the theoretical and experimental values show very good agreements.

The O–H out-of-plane bending band of No. 1 ring computed at 783 cm^{-1} (mode nos. 29, 28) slightly deviates from the observed band at 801 cm^{-1} in FT-IR, and it is higher than the literature value of $710\text{--}570\text{ cm}^{-1}$ [41]. This difference is due to the presence of intramolecular hydrogen bonding.

For isolated phenols, it has been shown that the frequency of O–H stretching vibration in the gas phase is about 3657 cm^{-1} [44,45]. In our case, the experimental wavenumber of 2924 cm^{-1} is assigned to O1–H stretching absorption due to the intramolecular hydrogen bonding effect, which is corresponding to the calculated value at 3058 cm^{-1} (mode no. 68). Comparing with the theoretical value of 3607 cm^{-1} (mode no. 75), a broad absorption peak observed at 3446 cm^{-1} ascribed to the O2–H stretching vibration is the evidence for the existence of intermolecular hydrogen bonds, which shows excellent agreements with literature data [44,46]. In addition, the hydrogen bonding results are also confirmed by a series of spectroscopic study of hydrogen bonds reported by Harold et al. [47].

5. Thermodynamic properties

On the basis of vibration analyses obtained by the frequency calculation at B3LYP/6-31G(d) level, the standard statistical thermodynamic functions, viz., heat capacities ($C_{p,m}^\ominus$), entropies (S_m^\ominus) and enthalpies (ΔH_m^\ominus) were obtained and listed in Table 5. The scale factor for frequencies is still 0.9614.

As seen from Table 5, all the values of heat capacities ($C_{p,m}^\ominus$), entropies (S_m^\ominus) and enthalpies (ΔH_m^\ominus) are increasing with temperatures ranging from 200.0 to 600.0 K, which is attributed to the enhancement of the molecular vibration while the temperature increases. The empirical correlations between the thermodynamic

Table 4
Experimental and calculated vibrational frequencies and approximate assignments for HPHBI^{a,b}.

Mode nos.	Experimental		Theoretical			Approximate assignments
	IR	Raman	Freq _i ^b	I _{IR}	S _{act}	
1			37	0.5	12.1	ωLattice
2			46	0.2	1.7	νLattice
3			67	0.3	2.5	ωLattice
4		117w	123	0.5	3.4	νLattice
5		145w	179	0.6	2.5	νLattice
6		212m	211	0.1	13.4	γC11O2+γC7N1
7		239w	214	1.4	18.5	γC1O1+γC7N1
8			277	0.4	1.0	γC7N1
9		341s	314	2.7	19.3	γC6C7N1
10			344	122.0	4.0	γO2H
11		444w	371	7.5	12.8	γN1C8+ωR ₂
12			396	2.5	2.8	βO2H
13		476s	411	3.0	17.4	γC-C of R ₂
14	453vw		437	7.1	0.6	βC1O1
15			455	1.4	2.5	γC-C of R ₁ +γCH of R ₁
16			479	2.0	3.1	βC-C of R _{1,2}
17	479m		501	19.9	0.2	γC-C of R ₂ +γCH of R ₂
18	525w	543m	524	15.8	3.9	γN1C8+γCH of R ₂
19	548w		541	1.5	1.4	γC-C of R ₁
20	574w	582m	553	2.2	10.1	βC-C of R ₁
21	620vw	630m	625	3.2	3.6	θR ₁
22	667vw		633	1.4	8.6	βC-C of R ₂
23			693	2.6	3.4	γC-C of R ₂
24			712	0.5	3.0	γC-C of R ₁
25	744m	737w	738	63.2	3.8	γCH of R ₁
26		770s	756	6.0	52.7	γCH of R ₂ +νC5-C6 of R ₁
27	766m		776	17.2	8.0	γCH of R ₂
28			783	69.5	0.8	γO1H
29	801vw		789	21.4	16.3	βC-C of R ₂ +γCH of R ₂ +γO1H
30			818	48.6	2.4	γCH of R ₂
31			837	0.1	4.6	γCH of R ₁
32	837vw	849ms	843	4.9	41.7	θR ₂ +βC-C of R ₁
33	852vw		882	10.0	4.0	γCH of R ₂
34			895	3.3	9.4	γCH of R ₂
35			903	1.1	5.0	γCH of R ₁
36			926	0.6	4.3	γCH of R ₂
37			943	0.3	0.1	γCH of R ₁
38	904w	1018w	963	7.4	54.9	γC7H
39			989	0.4	0.9	βR ₂ +βCH of R ₂
40		1045s	1020	3.9	49.7	βCH of R ₁ +νC-C of R ₁
41	1026w	1100m	1091	14.5	0.9	βCH of R ₂ +νC-C of R ₂
42			1103	7.4	1.6	βCH of R ₁ +νC-C of R ₁
43			1142	31.1	32.1	βCH of R ₁
44		1143m	1152	29.2	391.4	βCH of R ₂
45	1118w		1162	141.6	19.4	βO2H+νC-C of R ₂ +βCH of R ₂
46	1141vs	1165m	1176	135.6	683.3	νN1C8+νC6C7
47	1161w	1255ms	1213	12.6	193.0	βCH of R ₁ +βO1H
48			1232	1.8	29.0	βC7H+νC-C of R ₁ +βCH of R ₁
49	1224ms	1279m	1262	152.6	24.6	νC11O2+νC-C of R ₂ +βCH of R ₂
50	1244s		1282	6.5	31.9	βCH of R ₂ +νC-C of R ₂
51	1276s	1307m	1288	60.8	5.9	νC1O1+βC7H+βCH of R _{1,2}
52		1357vs	1322	0.1	239.5	νC-C of R ₁ +βCH of R ₁
53	1307s		1328	90.1	43.9	νC-C of R ₂ +βCH of R ₂ +βO2H
54	1371w	1371ms	1358	11.8	206.8	βC7H
55	1418w		1416	47.7	81.1	βO1H+βCH of R ₁
56			1430	20.3	13.5	νC-C of R ₂ +βCH of R ₂
57	1463vs	1514w	1456	68.5	922.7	νC-C of R ₁ +νC1O1
58	1487m		1489	66.5	52.8	νC-C of R ₁ +βCH of R ₁
59	1531ms	1525s	1500	163.3	467.2	νC-C of R ₂ +βCH of R ₂
60	1593s	1579w	1568	48.5	1495.7	νC-C of R ₁ +νC=N+βO1H
61			1579	13.3	0.5	νC-C of R ₂
62	1616w	1596ms	1597	33.8	3050.8	νC-C of R ₂
63			1618	19.3	27.2	νC-C of R ₁ +νC=N+βO1H
64	1633vs	1625s	1621	315.8	692.5	νC=N+νC-C of R _{1,2}
65	2855vw		2942	53.1	37.3	νC7H
66			3046	43.5	121.6	νCH of R ₂
67			3052	51.4	66.3	νCH of R ₁
68	2924vw		3058	379.6	83.3	νO1H+νCH of R ₁
69			3068	0.6	88.7	νCH of R ₁
70			3081	7.0	53.6	νCH of R ₂
71			3082	2.7	55.2	νCH of R ₂
72	3047w		3088	22.6	170.5	νCH of R ₁
73			3095	20.8	290.2	νCH of R ₁
74			3098	8.2	180.2	νCH of R ₂
75	3446b		3607	66.3	250.5	νO2H

^a Mode numbers are extracted from the output result of the B3LYP calculation;^b B3LYP scaled wavenumbers (cm⁻¹). I_{IR}: IR intensity (Kmmol⁻¹); S_{act}: Raman scattering activity (Kmmol⁻¹). s, strong; vs, very strong; m, medium; ms, medium strong; w, weak; vw, very weak; b, broad; R, ring (R₁: C1~C6, R₂: C8~C13); β, in-plane bending; γ, out-of-plane bending; ν, puckering; θ, breathing; ω, wagging; ν, stretching.

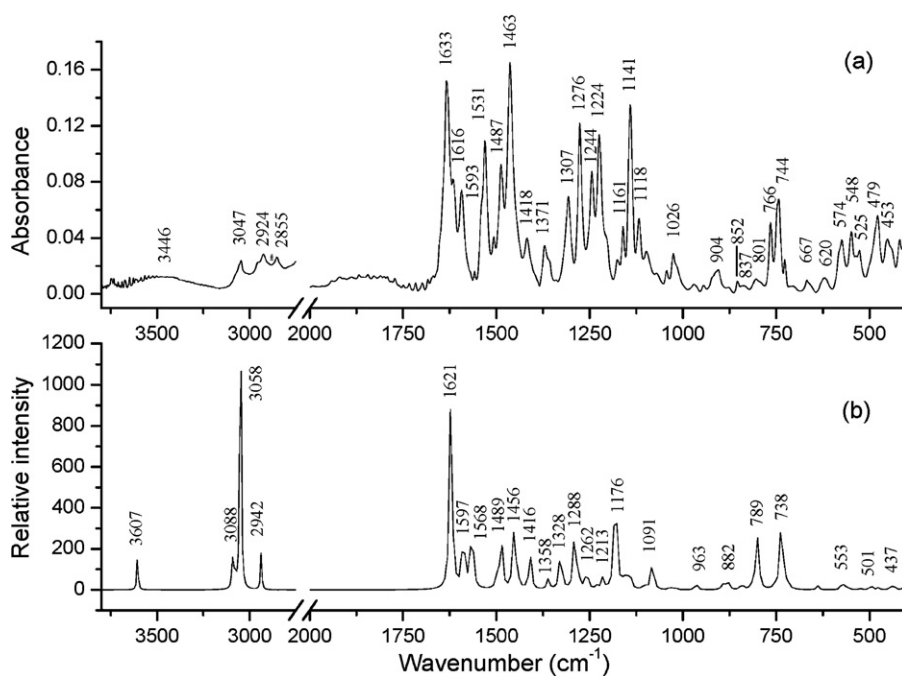


Fig. 3. IR spectra of HNBDI: (a) observed, (b) calculated.

Table 5

The thermodynamic parameters of HPHBI at different temperatures.

Temperature (K)	$C_{p,m}^{\ominus}$ (J/mol/K)	S_m^{\ominus} (J/mol/K)	ΔH_m^{\ominus} (kJ/mol)
200.0	158.02	405.31	18.19
250.0	195.97	444.64	27.04
298.2	232.15	482.26	37.35
300.0	233.52	483.70	37.78
350.0	269.22	522.41	50.36
400.0	302.15	560.54	64.65
450.0	331.94	597.88	80.52
500.0	358.57	634.26	97.80
550.0	382.29	669.56	116.33
600.0	403.42	703.75	135.98

parameters and temperatures are as follows (all the fitting factors are all beyond 0.999):

$$C_{p,m}^{\ominus} = -30.6562 + 1.0426T - 5.3022 \times 10^{-4}T^2 \quad (5)$$

$$S_m^{\ominus} = 258.8241 + 0.7481T \quad (6)$$

$$\Delta H_m^{\ominus} = -4.14540 + 0.0473T + 3.1165 \times 10^{-4}T^2 \quad (7)$$

All the thermodynamic data provide helpful information to further study on the title compound in the thermodynamic field.

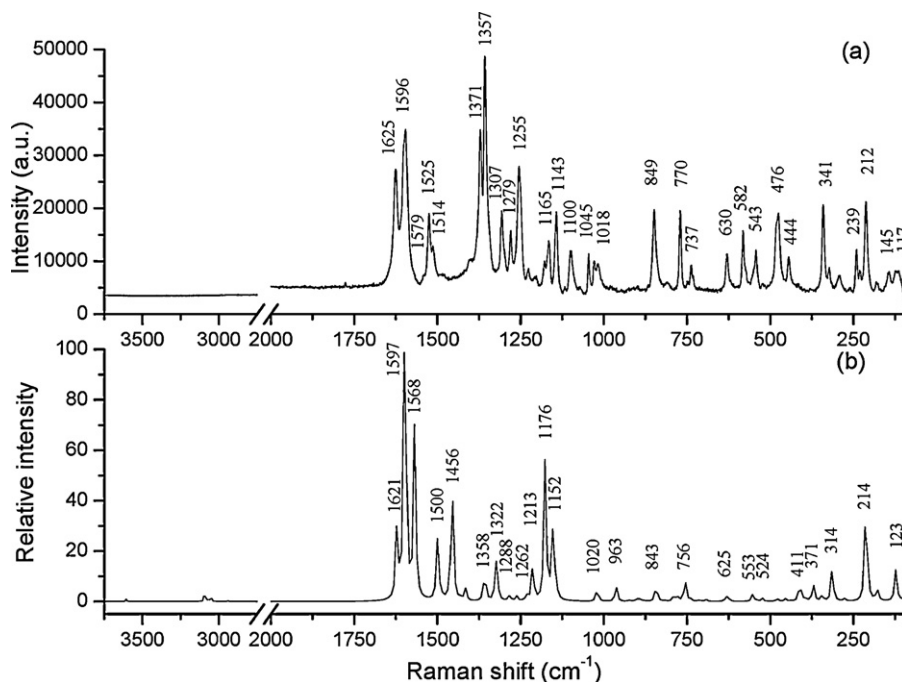
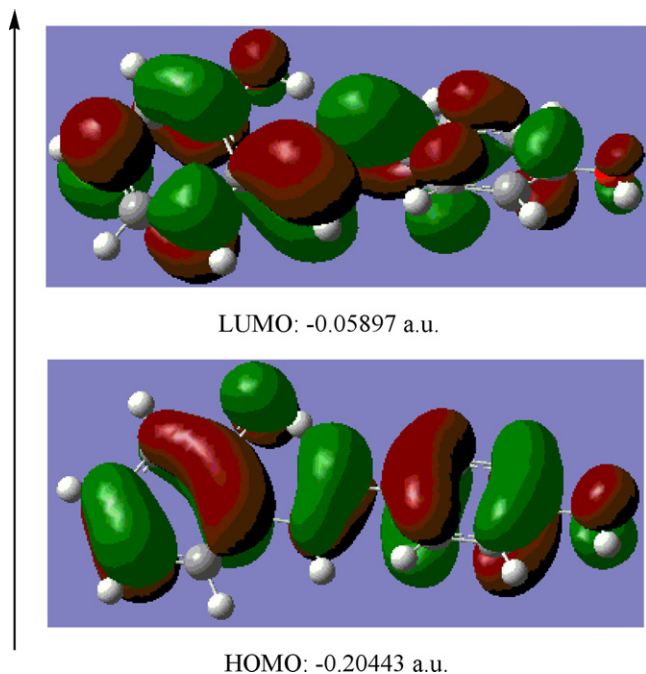


Fig. 4. Raman spectra of HNBDI: (a) observed, (b) calculated.

Table 6

The calculated electric dipole moments (Debye), static polarizability components (a.u.), first hyperpolarizability components (a.u.) of HPHBI.

μ_x	μ_y	μ_z	α_{xx}	α_{yy}	α_{zz}	β_{xxx}	β_{xxy}	β_{xyy}	β_{yyy}	β_{xxz}	β_{xyz}	β_{yyz}	β_{xzz}	β_{yzz}	β_{zzz}
0.44	-1.31	0.04	310.0	145.9	58.4	-1897.2	-214.1	6.6	-85.5	-119.6	-60.9	-17.8	4.9	-10.0	0.2

**Fig. 5.** Surfaces of FMOs for the studied molecule.

6. NLO properties

It is an important and inexpensive way to evaluate the NLO properties of materials by theoretical calculations. In order to understand the microscopic NLO mechanism of the title compound, we have applied Gaussian 03W program [21] to calculate electric dipole moment (μ), static polarizability (α) and first hyperpolarizability (β) components. All the calculated results were listed in Table 6. Then, the total static dipole moment (μ_0), average linear polarizability (α_0) and first-order hyperpolarizability (β_0) can be obtained by the calculations of the formula (2), (3) and (4). The corresponding values of μ_0 , α_0 and β_0 are 1.379 Debye, 25.378 Å³ and 1.655×10^{-29} cm⁵/esu, respectively. The α_0 and β_0 value of the investigated compound are all higher than those of urea ($\alpha_0 = 3.8312$ Å³, $\beta_0 = 3.7289 \times 10^{-31}$ cm⁵/esu). Theoretically, the first-order hyperpolarizability of the investigated compound is 44.4 times magnitude of urea, which is also larger than the values reported previously [3,32,35,48,49]. That is to say, the compound probably is a good candidate of NLO materials.

Many previous research works have indicated that the frontier molecular orbitals (FMOs) have significant effect on material NLO properties. In quest of the NLO characteristics, the surfaces of HOMO and LUMO of the studied molecule were shown in Fig. 5. We can see that the FMOs are composed of atomic p-electron orbitals and their electron clouds are easily polarized, which should be responsible for the NLO properties of the compounds.

7. Conclusions

In the present work, the studied compound was synthesized in one step by the condensation reaction of salicylaldehyde and 4-aminophenol in methanol solution. The crystal structure is confirmed by a single crystal XRD technique. The molecule adopts

trans configuration about central C=N bond with intramolecular hydrogen bonding, and the adjacent molecules form wave-shaped structure linked by strong intermolecular hydrogen bonding mechanism along *b* axis. The FT-IR and FT-Raman spectral bands are precisely assigned to its molecular structure with the aid of the theoretical calculations at B3LYP/6-31G(d) level, in which the experimental and theoretical results support each other. Furthermore, theoretical calculations give the thermodynamic and NLO properties for the compound. The total linear polarizability and first-order hyperpolarizabilities calculated respectively present 25.378 Å³ and 1.655×10^{-29} cm⁵/esu, which imply that the title compound might become a kind of good NLO material.

Acknowledgements

This work was supported by Natural Science Foundation of China (No. 21073092), Jiangsu Planned Projects for Postdoctoral Research Funds (No. 1001011C) and NUST Research Funding (No. 2010GJPY044). We also thank Qufu Normal University for Technical Assistance.

References

- [1] H. Ünver, A. Karakas, A. Elmali, Journal of Molecular Structure 702 (2004) 49–54.
- [2] A. Karakas, H. Ünver, Spectrochimica Acta Part A: Molecular and Biomolecular Spectroscopy 75 (2010) 1492–1496.
- [3] Y. Sun, Q. Hao, W. Wei, Z. Yu, L. Lu, X. Wang, Y. Wang, Journal of Molecular Structure: Theochem 904 (2009) 74–82.
- [4] Y. Sun, Q. Hao, Z. Yu, W. Wei, L. Lu, X. Wang, Molecular Physics 107 (2009) 223–235.
- [5] Y. Sun, Q. Hao, W. Wei, Z. Yu, L. Lu, X. Wang, Y. Wang, Journal of Molecular Structure 929 (2009) 10–21.
- [6] Y. Sun, W. Wei, Q. Hao, L. Lu, X. Wang, Spectrochimica Acta Part A: Molecular and Biomolecular Spectroscopy 73 (2009) 772–781.
- [7] H. Ünver, A. Karakas, A. Elmali, T.N. Durlu, Journal of Molecular Structure 737 (2005) 131–137.
- [8] E. Hadjoudis, M. Vittorakis, I. Moustakali-Mavridis, Tetrahedron 43 (1987) 1345–1360.
- [9] H. Ünver, T. Nuri Durlu, Journal of Molecular Structure 655 (2003) 369–374.
- [10] Y. Sun, Q. Hao, L. Lu, X. Wang, X. Yang, Spectrochimica Acta Part A: Molecular and Biomolecular Spectroscopy 75 (2010) 203–211.
- [11] Y. Sun, Q. Hao, Z. Yu, W. Jiang, L. Lu, X. Wang, Spectrochimica Acta Part A: Molecular and Biomolecular Spectroscopy 73 (2009) 892–901.
- [12] Y. Sun, R. Zhang, D. Ding, S. Liu, B. Wang, Y. Wang, Y. Lin, Structural Chemistry 17 (2006) 655–665.
- [13] R. Zhang, B. Du, G. Sun, Y. Sun, Spectrochimica Acta Part A: Molecular and Biomolecular Spectroscopy 75 (2010) 1115–1124.
- [14] R.R.B.N.K. Sethuraman, Spectrochimica Acta A 66 (2007) 707–711.
- [15] J.L. Chambers, K.L. Smith, M.R. Pressprich, Z. Jin, SMART, Bruker Advanced X-ray Solutions, Version 5.628, Bruker AXS Inc., Madison, WI, 2002.
- [16] SAINTPlus, Data Reduction and Correction Program, Version 6.22, Bruker AXS Inc., Madison, WI, 2001.
- [17] G.M. Sheldrick, SADABS, Program for Empirical Absorption Correction of Area Detector Data, University of Gottingen, Germany, 1996.
- [18] G.M. Sheldrick, SHELXS-97 and SHELXL-97; Programs for Structure Resolution and for Structure Refinement, University of Gottingen, Germany, 1997.
- [19] G.M. Sheldrick, SHELXTL, Structure Determination Software Suite, Version 6.10, Bruker AXS Inc., Madison, WI, 2000.
- [20] H. Arslan, O. Algul, T. Onkol, Spectrochimica Acta Part A: Molecular and Biomolecular Spectroscopy 70 (2008) 606–614.
- [21] M.J. Frisch, G.W. Trucks, H.B. Schlegel, G.E. Scuseria, M.A. Robb, J.R. Cheeseman, J.A. Montgomery Jr., T. Vreven, K.N. Kudin, J.C. Burant, J.M. Millam, S.S. Iyengar, J. Tomasi, V. Barone, B. Mennucci, M. Cossi, G. Scalmani, N. Rega, G.A. Petersson, H. Nakatsuji, M. Hada, M. Ehara, K. Toyota, R. Fukuda, J. Hasegawa, M. Ishida, T. Nakajima, Y. Honda, O. Kitao, H. Nakai, M. Klene, X. Li, J.E. Knox, H.P. Hratchian, J.B. Cross, C. Adamo, J. Jaramillo, R. Gomperts, R.E. Stratmann, O. Yazyev, A.J. Austin, R. Cammi, C. Pomelli, J.W. Ochterski, P.Y. Ayala, K. Morokuma, G.A. Voth, P. Salvador, J.J. Dannenberg, V.G. Zakrzewski, S. Dapprich, A.D. Daniels, M.C. Strain, O. Farkas, D.K. Malick, A.D. Rabuck, K. Raghavachari, J.B. Foresman, J.V. Ortiz, Q. Cui, A.G. Baboul, S. Clifford, J. Cioslowski, B.B. Stefanov, G. Liu, A. Liashenko, P. Piskorz, I. Komaromi, R.L. Martin, D.J. Fox, T. Keith, M.A. Al-Laham,

- C.Y. Peng, A. Nanayakkara, M. Challacombe, P.M.W. Gill, B. Johnson, W. Chen, M.W. Wong, C. Gonzalez, J.A. Pople, Gaussian 03W, Version 6. 0, Gaussian Inc., Wallingford, CT, 2004.
- [22] R. Dennington II, T. Keith, J. Millam, K. Eppinnett, W. Lee Hovell, R. Gilliland, GaussView, Version 3. 09, Semichem, Inc., Shawnee Mission, KS, 2003.
- [23] V. Krishnakumar, G. Keresztury, T. Sundius, R. Ramasamy, *Journal of Molecular Structure* 702 (2004) 9–21.
- [24] P.L. Polavarapu, *Journal of Physical Chemistry* 94 (1990) 8106–8112.
- [25] A. Karakas, A. Elmali, H. Ünver, I. Svoboda, *Spectrochimica Acta Part A: Molecular and Biomolecular Spectroscopy* 61 (2005) 2979–2987.
- [26] P.S. Liyanage, R.M. de Silva, K.M.N. de Silva, *Journal of Molecular Structure: Theochem* 639 (2003) 195–201.
- [27] P.J. Mendes, J.P.P. Ramalho, A.J.E. Candeias, M.P. Robalo, M.H. Garcia, *Journal of Molecular Structure: Theochem* 729 (2005) 109–113.
- [28] I.C. de Silva, R.M. de Silva, K.M. Nalin De Silva, *Journal of Molecular Structure: Theochem* 728 (2005) 141–145.
- [29] J.O. Morley, *Journal of American Chemical Society* 110 (1988) 7660–7663.
- [30] H. Li, K. Han, X. Shen, Z. Lu, Z. Huang, W. Zhang, Z. Zhang, L. Bai, *Journal of Molecular Structure: Theochem* 767 (2006) 113–118.
- [31] A.D. Tillekaratne, R.M. de Silva, K.M.N. de Silva, *Journal of Molecular Structure: Theochem* 638 (2003) 169–176.
- [32] D. Sajan, H. Joe, V.S. Jayakumar, J. Zaleski, *Journal of Molecular Structure* 785 (2006) 43–53.
- [33] H. Alyar, Z. Kantarci, M. Bahat, E. Kasap, *Journal of Molecular Structure* 2007 (2007) 516–520.
- [34] N. Sundaraganesan, J. Karpagam, S. Sebastian, J.P. Cornard, *Spectrochimica Acta Part A: Molecular and Biomolecular Spectroscopy* 73 (2009) 11–19.
- [35] K.S. Thanthiriwatte, K.M. Nalin de Silva, *Journal of Molecular Structure: Theochem* 617 (2002) 169–175.
- [36] C.C. Ersanli, C. Albayrak, M. Odabasoglu, A. Erdonmez, *Acta Crystallographica Section E* 60 (2004) o389–o391.
- [37] M. Dolaz, V. McKee, M. Köse, A. Gölcü, M. Tümer, *Spectrochimica Acta Part A: Molecular and Biomolecular Spectroscopy* 77 (2010) 219–225.
- [38] M. Karabacak, E. Şahin, M. Çınar, I. Erol, M. Kurt, *Journal of Molecular Structure* 886 (2008) 148–157.
- [39] A.P. Scott, L. Radom, *Journal of Physical Chemistry* 100 (1996) 16502–16513.
- [40] J. Swaminathan, M. Ramalingam, V. Sethuraman, N. Sundaraganesan, S. Sebastian, *Spectrochimica Acta Part A: Molecular and Biomolecular Spectroscopy* 73 (2009) 593–600.
- [41] L. Guru Prasad, V. Krishnakumar, R. Nagalakshmi, *Physica B* 405 (2010) 1652–1657.
- [42] N. Sundaraganesan, H. Saleem, S. Mohan, M. Ramalingam, *Spectrochimica Acta Part A: Molecular and Biomolecular Spectroscopy* 61 (2005) 377–385.
- [43] M. Ilic, E. Koglin, A. Pohlmeier, H.D. Narres, M.J. Schwuger, *Langmuir* 16 (2000) 8946–8951.
- [44] D. Michalska, D.C. Bienko, A.J. Abkowitz-Bienko, Z. Latajka, *The Journal of Physical Chemistry* 100 (1996) 17786–17790.
- [45] G.V. Hartland, B.F. Henson, V.A. Ventura, P.M. Felker, *The Journal of Physical Chemistry* 96 (1992) 1164–1173.
- [46] S. Sebastian, N. Sundaraganesan, S. Manoharan, *Spectrochimica Acta Part A: Molecular and Biomolecular Spectroscopy* 74 (2009) 312–323.
- [47] H.H. Freedman, *Journal of American Chemical Society* 83 (1961) 2900–2905.
- [48] C. Ravikumar, I.H. Joe, V.S. Jayakumar, *Chemical Physical Letters* 460 (2008) 552–558.
- [49] F.F. Jian, P. Zhao, L. Zhang, J. Zheng, *Journal of Fluorine Chemistry* 127 (2006) 63–67.